PHYSICAL REVIEW C VOLUME 51, NUMBER 5 MAY 1995

Study of baryon resonances through $\gamma p \rightarrow \eta p$ differential cross sections

S. A. Dytman, W. W. Daehnick, J. G. Hardie,* and M. Yamazaki†
Department of Physics and Astronomy, University of Pittsburgh, Pittsburgh, Pennsylvania 15260

E. Booth and J. Miller
Department of Physics, Boston University, Boston, Massachusetts 02215

M. J. Leitch, C. S. Mishra,‡ and J. C. Peng
Physics Division, Los Alamos National Laboratory, Los Alamos, New Mexico 87545

D. R. Tieger and K. F. von Reden§
Bates Linear Accelerator and Department of Physics, Massachusetts Institute of Technology, Middleton, Massachusetts 01949
(Received 28 November 1994)

We present new data for the $\gamma p \rightarrow \eta p$ reaction at average photon energies of 729 and 753 MeV. The reaction is believed to be dominated by intermediate states of N^* resonances and should be an excellent way to study the internal structure of the baryon states. Previously published data were consistent with a dominance of the $S_{11}(1535)N^*$ resonance intermediate states in the reaction mechanism. The new data show deviations from this picture for the first time.

PACS number(s): 13.60.Rj, 14.20.Gk

I. INTRODUCTION

The microscopic structure of baryons is a subject of great interest as a testing ground for models of the strong interaction. For many years, the existence of many excited states of the proton has been known [1]. The success in describing the basic properties of these states (e.g., spins, parities, masses, and magnetic moments) has long been a strong argument in favor of quark models. Experiments at high energy have provided considerable evidence for quantum chromodynamics (QCD) as the correct microscopic theory of strong interactions. These experiments test the short-range character of the force where the coupling is weak and perturbation theory can be used. To describe the long-distance behavior, the coupling parameters are quite large and solutions to QCD problems are much more difficult to obtain. Although it is based largely on empirical evidence, the nonrelativistic quark model (NRQM) has been quite successful in both describing and predicting properties such as those listed above.

The photon coupling strengths for transitions between the baryon ground states (proton and neutron) and the excited states are an excellent test of the baryon wave functions that quark models produce. The coupling strength is often expressed in terms of the $\gamma N \rightarrow N^*$ matrix element labeled by total helicity; $A_{1/2}$ and $A_{3/2}$ are the appropriate helicity amplitudes for real photons. The experiments required to measure these quantities are quite difficult and the information is far from complete as of now. Nevertheless, the NRQM has had significant success in describing existing data for these more detailed properties [2].

A major part of the difficulty in measuring the helicity amplitudes accurately comes from the need to accumulate a large data base in order to unambiguously identify the strength of excitation for each excited baryon state. Because the states all decay via the strong interaction to a baryon plus mesons, the final state is complicated. Although the states are clustered in three regions of mass (centered at about 1240, 1520, and 1700 MeV), they are wide and overlapping. Therefore, the extraction of partial wave amplitudes [e.g., Chew-Goldberger-Low-Nambu (CGLN) multipoles [3]] is complicated, but absolutely necessary.

We can get information on the N^* states by taking advantage of the selectivity that occurs when the final state contains only one meson which is an η. Because the η is an isoscalar particle, only isospin $\frac{1}{2}$ baryons (N^*'s) can decay into ηN. This excludes all isospin $\frac{3}{2}$ states, e.g., Δ's. There is good empirical evidence that very few N^*'s have a strong decay branch to ηN, with the $S_{11}(1535)$ being one of only two resonances [the other is $P_{11}(1710)$] with a branching ratio larger than 6% in the latest review [1]. Before the experiment reported here, only 192 differential cross section and 12 polarization data points for the $\gamma p \rightarrow \eta p$ reaction were published for total center-of-mass energy (W) less than 2.2 GeV. Most of these data were taken more than twenty years

*Present address: Physics Department, University of Indiana, Bloomington, IN 47405.

†Present address: Mitsubishi Electric Corporation, Nuclear Energy Section, Tokyo, Japan.

‡Present address: Accelerator Department, Fermi National Accelerator Laboratory, Batavia, IL 60510.

§Present address: Woods Hole Oceanographic Institute, Woods Hole, MA.

ago, and many experiments used the difficult technique of bremsstrahlung subtraction. There were also a few electroproduction measurements which give the best evidence for the selectivity of final states involving η-nucleon to the $S_{11}(1535)$, one of the strongly excited states in the second resonance region. The best signature of this resonance to date has been seen in the electroproduction experiments at low Q^2 [4]. The angular distributions are isotropic within errors ($\sim \pm 10\%$) and the total center-of-mass energy dependence matches the Breit-Wigner shape with proper threshold dependence. Isotropic angular distributions are expected for an S_{11} intermediate state because it must be excited through the E_{0+} multipole.

The real photon experiments have been less conclusive on the nature of the $S_{11}(1535)$ because the necessary data are nonexistent or of low quality. This is particularly true close to threshold ($W = 1487.1$ MeV or $E_\gamma = 709.3$ MeV). There are angular distributions at photon beam energies of ~ 800 MeV ($W = 1543$ MeV) [5,6] and ~ 750 MeV ($W = 1513$ MeV) [6], and two data points with 20% statistical error at ~ 725 MeV ($W = 1497$ MeV) [6]. The latter two data sets are shown below. The main purpose of the present experiment was to measure differential cross sections close to threshold to investigate the S_{11} dominance. Other resonances [e.g., $P_{11}(1440)$ or $D_{13}(1520)$] can contribute, but sensitivity has been low in previous experiments. With better data, we will have improved capability to extract the photon and η coupling parameters to these low-lying resonances, neither of which are well understood at present.

II. EXPERIMENT

This experiment was done at the real photon line at the MIT-Bates Linear Accelerator. Close to threshold the η's that must be detected are of very low energy and the short η lifetime prevents direct detection. We chose to detect the η through the decay to $\gamma\gamma$ (38.9% branching ratio). The two photons then have large opening angle and invariant mass equal to the η mass, with each photon having energy of about half the η mass. For this experiment, the beam photons had a bremsstrahlung spectrum with end-point energy 768 MeV. Thus, only the beam photons of energy 709.3–767.5 MeV were able to initiate the reaction of interest. The minimum opening angle of the decay photons that had to be detected was 99.1°. Two arrays were constructed for photon detection, each array consisting of 24 lead glass blocks of area 19.1×19.1 cm and thickness 30.5 cm. The detectors were positioned in three geometries about the liquid hydrogen target allowing detection of η's from the desired reaction at all angles for all photon beam energies from threshold to 768 MeV. The target was 10.16 cm thick; after collimation, the beam spot was measured to be about 1.5 cm in diameter at the target.

Although the apparatus had a large solid angle (integrated value of about 0.25 sr for each setting), the energy resolution was moderate. The energy resolution of the decay photons in the lead glass detectors was about 20% FWHM at 300 MeV and the η mass resolution was about 130 MeV FWHM. Both η energy and scattering angle measurements depend more on the position data for photon hits within the arrays than the data for the deposited energy. At a radius of 1.25 m from the target, the laboratory scattering angle resolution was 2° for η's, corresponding to 10° for the center-of-mass angle. The incident γ energy was calculated for each event from the measured values of η energy and angle. Although there was no way to directly measure the error in this determination of photon beam energy, Monte Carlo calculations give an expected error of 12 MeV and the data are compatible with this value. The incident photon distribution was divided into two bins, 709–740 and 740–768 MeV. The weighted average energies for each of these energy ranges are 729 ± 5 and 753 ± 5 MeV, respectively. Differential cross sections were determined for each of these ranges of beam energy.

A Monte Carlo code was used to calculate the η resolutions and acceptance. It was checked by matching to published π^0 distributions [7]. The differential cross section for the $\gamma p \rightarrow \pi^0 p$ reaction was measured with the same apparatus as was used for the (γ, η) data; however, the central center-of-mass scattering angle of the apparatus was 89° and the electron beam energy was 328 MeV. To get agreement with the Bonn data [7], all cross sections in this experiment had to be renormalized by a factor of 1.11, consistent with the estimated absolute error in this experiment. The quoted absolute error for the Bonn data are $\pm 5\%$. The incident photon intensity was monitored with a quantameter which has been calibrated to an accuracy of about 3% for all energies of this experiment [8]. The lead glass blocks were calibrated in energy with a low intensity electron beam and monitored throughout the experiment with cosmic rays. The electron beam energy was determined with an accuracy of ± 4 MeV through elastic electron scattering spectra measured with a magnetic spectrometer using the same beam. Since the product of the total cross section and bremsstrahlung flux are approximately constant over the energies of this experiment, the error in electron beam energy introduces an error no larger than a few percent into the final cross sections.

There were two major backgrounds in the experiment for which corrections were made to the cross sections. With a duty cycle of 1%, the beam intensity had to be low (average rate of 1.3×10^6 Hz for photons above η threshold) to keep the random coincidence rate less than 20% of the on-line data rate. The contribution from these events was monitored in conjunction with the real data collection by using a wide coincidence gate for the hardware trigger. These events were distributed randomly within the gate. This source of background was fit to a flat distribution and subtracted in the offline analysis. After cuts, the largest correction made due to this source was 9.4%. Events from correlated photons produced via the reaction $\gamma p \rightarrow \pi^0 \pi^0 p$ were unable to be detected by timing. Their contribution had to be computed by Monte Carlo calculation. Four photon events were generated according to phase space decays of a $\Delta^+ \pi^0$ state (uncorrelated three particle phase space events gave a very similar result) and the detectors were checked for two photon combinations that would have high invari-

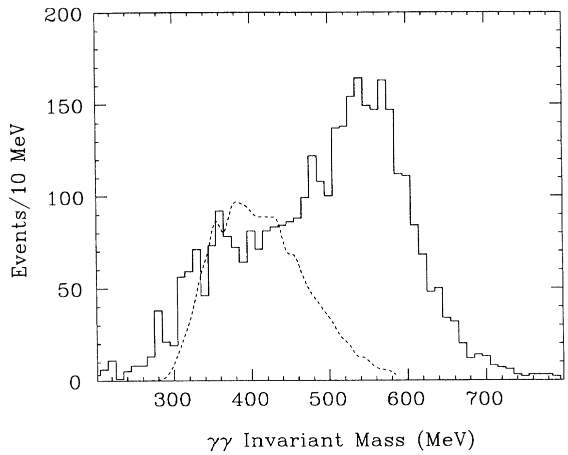

FIG. 1. The invariant mass of photon pairs after random background has been subtracted for the detector configuration with the arrays at 74° and −38°. The dashed line is the background contribution for $\pi^0\pi^0$ events as calculated by a Monte Carlo program.

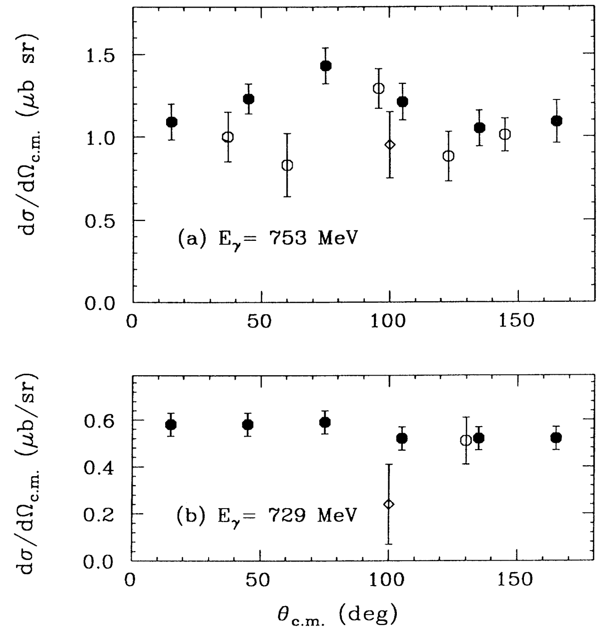

FIG. 2. Differential cross section data for this experiment at average photon beam energies of 753 MeV [solid dots in (a)] and 729 MeV [solid dots in (b)]. Older data from Prepost *et al.* [6] are shown as diamonds and older data from Delcourt *et al.* [6] are shown as open circles.

ant mass. One of the invariant mass distributions from the experiment is shown in Fig. 1 along with the calculated $2\pi^0$ background. The magnitude of the background was consistent with the published total cross sections for the reaction. Although the simulation does not agree in detail with the shape of the background in the data, care was taken to maintain a consistent and symmetric shape in the background-subtracted invariant mass distribution. The same Monte Carlo events were then used to generate the $2\pi^0$ contribution to each point in the angular distribution, using the same cuts as were applied to the actual data. A correction was made for each angle bin, ranging in value between 1% and 12%. The largest corrections were made to the forward angle bins at the higher photon beam energy. A small contribution was made to the overall error bar for possible errors in this correction. Another possible source of background was events from the target containment structure. This background was measured by emptying the liquid hydrogen target and taking data in the geometry with the highest background. Since the background event rate was less than 1% of the rate seen with a full target, no correction was made.

The new data are presented at average photon energies of 729 and 753 MeV in Fig. 2 where they are compared to previous data [6]. With the large solid angle coverage of the apparatus, most of the new data points are an average of two or three separate measurements (same detectors, but different geometry). The consistency among these separate measurements provides strong evidence that the Monte Carlo acceptances are accurate. The error bars include both statistical and Monte Carlo sources. A contribution to the estimated error for each cross section measurement due to Monte Carlo of 5% was added in quadrature with the estimated statistical error.

Previously published data are plotted as diamonds and open circles in Fig. 2. The old data at the lower beam energy established only the general level of cross section, which is consistent with the new data. At the higher beam energy, the new cross sections are about 20% larger than the 1960s data; although the new data may suggest a small peak at about 90°, the older data have uncertainties that obscure any structure at the 20% level. The absolute normalization error in the new data is estimated to be ±10%.

III. PHENOMENOLOGICAL ANALYSIS

Because the data are close to threshold, they can usefully be analyzed in terms of Legendre polynomials $P_L(x)$ with $x = \cos\theta_{\text{c.m.}}$. If the intermediate state is $S_{11}(1535)$ or $P_{11}(1440)$ alone, only the E_{0+} or M_{1-} multipoles (respectively) can be populated and the angular distribution will be isotropic in both cases. If the reaction is dominated by the $D_{13}(1520)$, a mixture of E_{2-} and M_{2-} multipoles will be seen and the angular distribution will be combination of P_0 and P_2. Nonresonant terms will give contributions of P_0, P_1, and perhaps P_2. Of course, any of these reaction amplitudes can interfere. We fit each angular distribution for W less than 1.7 GeV by the function

$$s(\theta_{\text{c.m.}}) = aP_0 + bP_1(x) + cP_2(x) \ .$$

The fitted values of b and c ($L = 1, 2$) are much smaller than that of a ($L = 0$) and are statistically consistent with zero except in the case of the new 753 MeV data. The fitted total cross section is equal to $4\pi a$ and is plotted

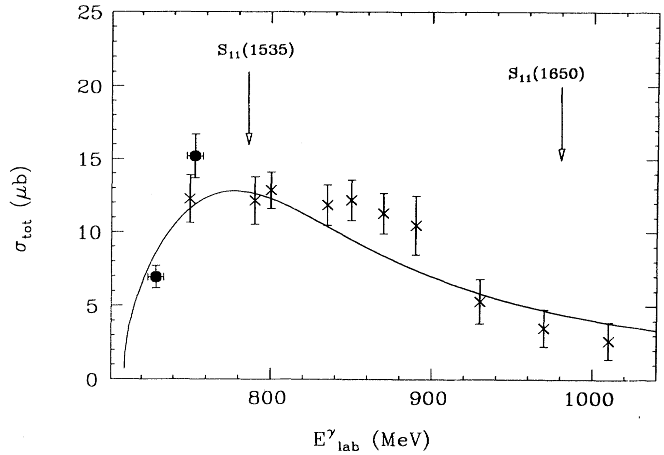

FIG. 3. Total cross section data from Legendre polynomial fits to η photoproduction data for a proton target. The solid dots are results from this experiment and the $\times$'s are from previous experiments. See text for details.

in Fig. 3. Errors shown include the fitting error added in quadrature with experimental systematic error. The new data are plotted as filled circles.

At this point, the role of the $S_{11}(1535)$ resonance can already be estimated. If the data were solely due to an intermediate state of this resonance, the angular distributions would be isotropic and the energy dependence would be that of a Breit-Wigner with proper threshold dependence. The 729 MeV distribution is flat within the accuracy of this experiment and the 753 MeV data have a mild peak at about 90°. The data point with the largest cross section is for the higher beam energy at 75°. The differential cross section at that angle was measured in three different geometries, giving values of 1.39 ± 0.07, 1.47 ± 0.07, and 1.40 ± 0.21 μb/sr. For these three measurements, the sizes of the $2\pi^0$ background corrections were 8.2%, 6.8%, and 1.1%, respectively. Thus, the data are internally consistent, leading to the qualitative conclusion that the S_{11} contribution is probably significant, but not totally dominant.

The energy dependence of the total cross section data and the Breit-Wigner shape (mass of 1535 MeV and full width of 150 MeV [1] were used) are shown in Fig. 3. Previous data have the largest cross section at 800 MeV (W = 1543 MeV), an average of about 1.1 μb/sr. We chose to fix the amplitude of the Breit-Wigner shape to the 800 MeV data. The energy dependence of previous data is roughly a Breit-Wigner distribution and has been taken in the past as evidence for dominance of $S_{11}(1535)$ [6]. With the normalization chosen, the average cross section should be 0.94 μb/sr at 753 MeV and 0.68 μb/sr at 729 MeV. Including the estimated absolute errors, this simple prediction is about one standard deviation larger than the new data at the beam energy of 729 MeV, and about two standard deviations less than the average cross section at 753 MeV. The ratio of the total cross sections at the two energies would be 1.4 for S_{11} dominance; however, the ratio is 2.2 ± 0.2 in this experiment. The older 750 and 775 MeV data are consistent with what would be expected for S_{11} dominance, but with poorer accuracy. Although the total cross section data for η photoproduction are strongly peaked at W of roughly 1535 MeV, it is two standard deviations larger for the new data (W = 1514 MeV) than the previous data is 1543 MeV as discussed above. Since there is unlikely to be any cause for a sharp energy dependence in this reaction, we conclude that the new cross section data are inconsistent with the previous data at higher energies. The energy dependence of the new data is not in good agreement with the expectations of pure S_{11} excitation even if the magnitude of the Breit-Wigner shape in Fig. 3 is allowed to float.

IV. ISOBAR FITTING ANALYSIS

We have made fits to $\gamma p \to \eta p$ data using an isobar model very similar to one of the simpler models used by the Particle Data Group (PDG) [1] in the presently accepted helicity amplitude analysis of baryon resonance data. The computer code used was an extension of work done previously by Tabakin, Dytman, and Rosenthal [9]. The differential cross section and polarization data are fit to CGLN multipoles [3]. Each known resonance in Ref. [1] contributes to the appropriate multipoles (just 1 multipole for S_{11} and P_{11}, 2 for resonances of higher spin) with a Breit-Wigner energy dependence including appropriate barrier penetration factors. The resonance mass, full width, and branching ratio to ηN are taken from Ref. [1]. Nonresonant contributions calculated from Born amplitudes are included in the E_{0+} and M_{1-} multipoles. This model is a simple way to parametrize the primary reaction mechanism, but is not necessarily unitary or crossing symmetric.

Since the new data focus on the region close to threshold, we only used data for photon beam energies less than 1 GeV (a total of 81 data points previous to this experiment) for these fits. The resonances in the second resonance region [$S_{11}(1535)$, $D_{13}(1520)$, and $P_{11}(1440)$] are expected to be the strongest contributors, although tails from higher lying states must be included. Each known resonance was parametrized by the electric and/or magnetic coupling strength for each allowed multipole and a relative phase. These strengths are a product of the photon helicity amplitude discussed in the Introduction and the $N^* \to N\eta$ decay width. At present, values for the latter are taken from $\pi^- p \to \eta n$ data; the sign of the fit helicity amplitude is therefore ambiguous and is ignored here. Photon helicity amplitudes and phases for the three second resonance region resonances were fit (seven parameters). Helicity amplitudes for the remaining five resonances expected to contribute were fixed to the PDG values [1]. Relative phases for these five resonances were also fit; in fact, no fit is possible without the freedom of choosing these phases freely. A total of 12 parameters was determined by the fit. Results given here are all obtained keeping the nonresonant amplitude constant; when those amplitudes were fit, none of the results changed. The fit cross sections are dominated by the $S_{11}(1535)$. Using only the $\gamma N \to \eta N$ data previous to this experiment, the S_{11} helicity amplitude is determined to be $A_{1/2} = 0.063 \pm 0.009$ GeV$^{-1/2}$, compared to the PDG value of 0.074 ± 0.011 GeV$^{-1/2}$ which was based totally on πN elastic and $\gamma N \to \pi N$ data. This coupling is sensitive to the S_{11} total width which is somewhat uncertain in the PDG summary. The other fit helicity amplitudes differ substantially from the PDG values, but are probably not significant. When the best-fit function is extrapolated to threshold, the calculated cross sections are about two standard deviations away from the new data (see Fig. 3).

When the new data are included, the fits get worse. While the fits discussed in the previous paragraph had χ^2 per degree of freedom equal to about 2.0, the new fits generate χ^2/df of about 3.3. This is likely due to the incompatibility of the new and older data sets. The best-fit helicity amplitude for the dominant resonance, $S_{11}(1535)$, increases to 0.066 ± 0.013 GeV$^{-1/2}$ when the new data are included.

V. PREVIOUSLY PUBLISHED THEORETICAL CALCULATIONS

Fits to the η photoproduction data were also made by Benmerrouche and Mukhopadhyay [10] using just the data previous to this experiment, but with a better model than is presented above. They used an effective Lagrangian model which has correct symmetry properties built in to some extent and phases are predicted rather than fit. Their results for the helicity amplitudes are qualitatively similar to those of the fitting exercise described above, except the $S_{11}(1535)$ helicity amplitude is 0.095 ± 0.011 GeV$^{-1/2}$. Their results for 753 and 729 MeV are shown in Fig. 4 as dashed lines. The angular distributions are quite flat and about 10% less than the values expected from a model dominated by the S_{11}. A criticism that can be made of both these fitting models is the lack of information about pion photoproduction used.

There was one theoretical prediction (Bennhold and Tanabe [11]) for these data before they were analyzed. This analysis fits the data for pion photoproduction from the nucleon, pion-nucleon scattering, and $\pi^- p \to \eta n$ in a coupled-channel model, parametrizing all the information needed to calculate η photoproduction from the nucleon. They leave out all resonances at higher mass than 1535 MeV, so the model is only valid at energies close to threshold. The predictions from this model are shown as solid lines in Fig. 4. The energy dependence is quite different than a model with S_{11} dominance, indicating significant contributions from non-$S_{11}(1535)$ mechanisms. The data do show non-S_{11} features, but to a much smaller extent than those predicted by Bennhold and Tanabe.

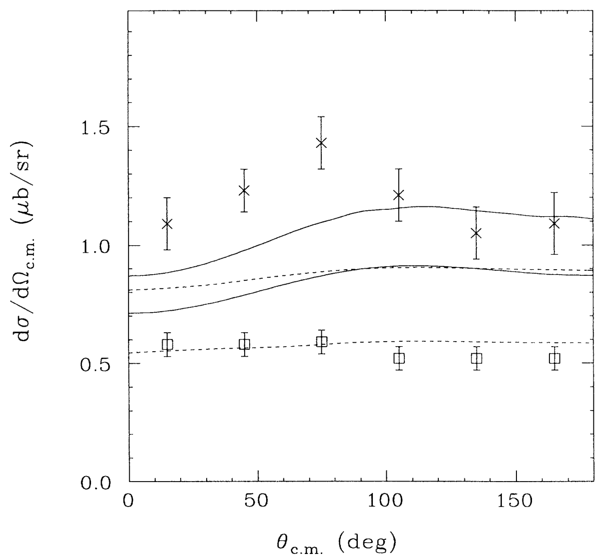

FIG. 4. Differential cross section data for this experiment at 753 MeV (×'s) and 729 MeV (boxes). Also shown are the predictions at these energies from the model of Bennhold and Tanabe [11] (solid lines) and the predictions based on fits to previous η data due to Benmerrouche and Mukhopadhyay [10] (dashed lines). For each set of lines, the upper curve is for the larger beam energy.

In summary, we have presented new data for the $\gamma p \to \eta p$ reaction, the most accurate data close to threshold published so far. Qualitative analysis shows that the earlier interpretation of this reaction as dominated by intermediate $S_{11}(1535)$ states is largely correct, but modifications to this picture are now needed. From the energy dependence, the absolute level of the 753 MeV cross sections in this experiment is incompatible with the previous data at about 800 MeV [5]. The Bennhold and Tanabe prediction [11] is not in good agreement with the new data.

Note added in proof: We have recently learned of a paper [J. Price *et al.*, Phys. Rev. C **51**, 2283 (1995)] which gives new data for total cross sections very close to the threshold for the same process. Their data are consistent with the pure S_{11} intermediate state.

ACKNOWLEDGMENTS

The authors are grateful to the University of British Columbia group for allowing us to use their lead-glass detectors and to Helmut Baer (LAMPF) for providing us with the computer code from which the acceptance code for this experiment was developed.

[1] Particle Data Group, Phys. Rev. D **45**, 1 (1992).
[2] S. Capstick, Phys. Rev. D **46**, 2864 (1992).
[3] G. F. Chew, M. Goldberger, F. Low, and N. Nambu, Phys. Rev. **106**, 1345 (1957).
[4] H. Breuker *et al.*, Phys. Lett. **74B**, 409 (1978); U. Beck *et al., ibid.* **51B**, 103 (1974).
[5] C. Bacci, R. Baldini-Celio, C. Mencuccini, M. Spinetti, and A. Zallo, Phys. Rev. Lett. **20**, 571 (1968); S. Homma, M. Kanazawa, K. Maruyama, H. Okuno, A. Sasaki, and T. Taniguchi, J. Phys. Soc. Jpn. **57**, 828 (1988).

[6] R. Prepost, D. Lundquist, and D. Quinn, Phys. Rev. Lett. **18**, 82 (1967); B. Delcourt, J. Lefrancois, J. P. Perez-Y-Jorba, G. Sauvage, and G. Mennessier, Phys. Lett. **29B**, 75 (1969).

[7] H. Genzel, E. Hilger, G. Knop, H. Kemen, and R. Wedemeyer, Z. Phys. **268**, 19 (1974).

[8] D. R. Tieger, E. C. Booth, J. P. Miller, B. L. Roberts, J. Commuzzi, G. W. Dodson, S. Gilad, and R. P. Redwine, Phys. Rev. Lett. **53**, 755 (1984).

[9] F. Tabakin, S. Dytman, and A. Rosenthal, in *Excited Baryons 88*, Proceedings of the Topical Workshop on Excited Baryons, Troy, NY, edited by G. Adams, N. C. Mukhopadhyay, and P. Stoler (World Scientific, Singapore, 1989), p. 168.

[10] M. Benmerrouche and N. Mukhopadhyay, Phys. Rev. Lett. **67**, 1070 (1991); (private communication).

[11] C. Bennhold and H. Tanabe, Nucl. Phys. **A350**, 625 (1991); (private communication).